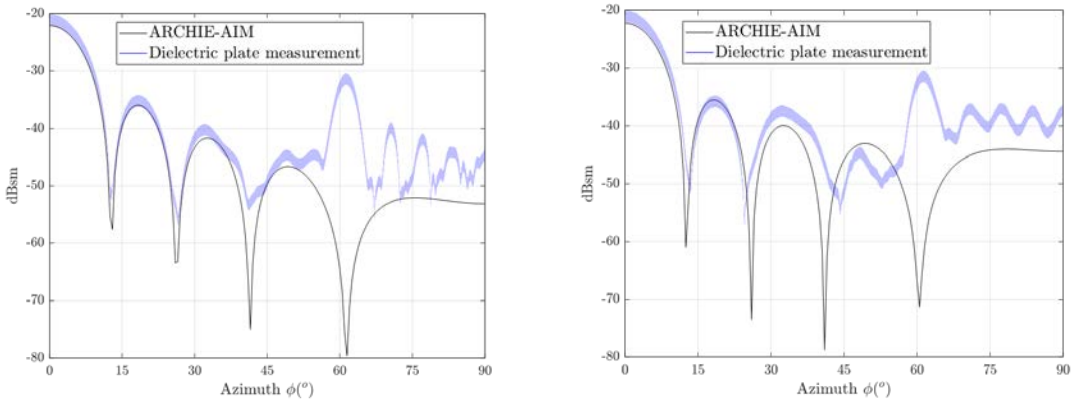

Figure 1: The HH ($\sigma_{\phi\phi,\mathrm{dB}}$, left) and VV ($\sigma_{\theta\theta,\mathrm{dB}}$, right) polarized RCS for the thin dielectric plate of width W = 6 in at frequency f = 2.56 GHz.

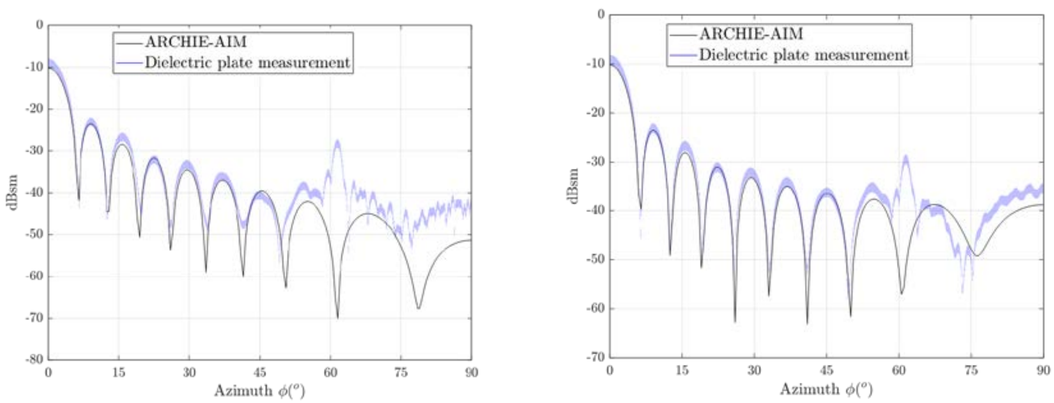

Figure 2: The HH ($\sigma_{\phi\phi,\mathrm{dB}}$, left) and VV ($\sigma_{\theta\theta,\mathrm{dB}}$, right) polarized RCS for the thin dielectric plate of width W = 6 in and frequency f = 5.12 GHz.

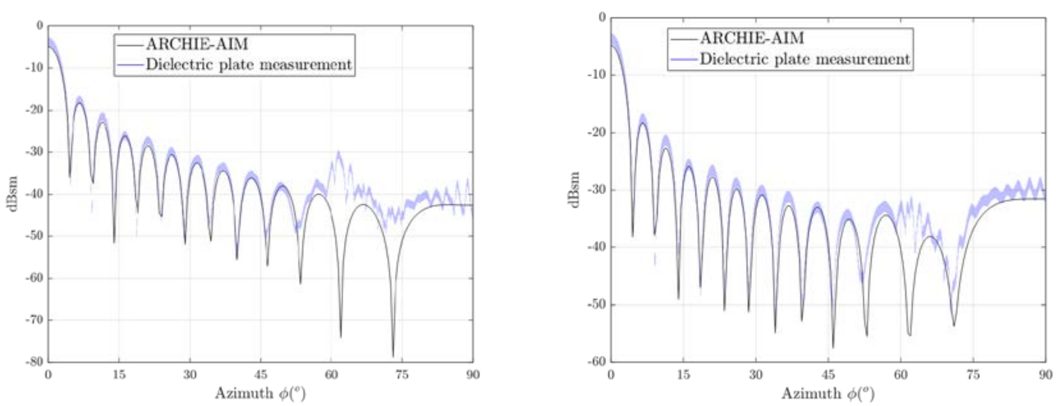

Figure 3: The HH ($\sigma_{\phi\phi,\mathrm{dB}}$, left) and VV ($\sigma_{\theta\theta,\mathrm{dB}}$, right) polarized RCS for the thin dielectric plate of width W = 6 in and frequency f = 7 GHz.

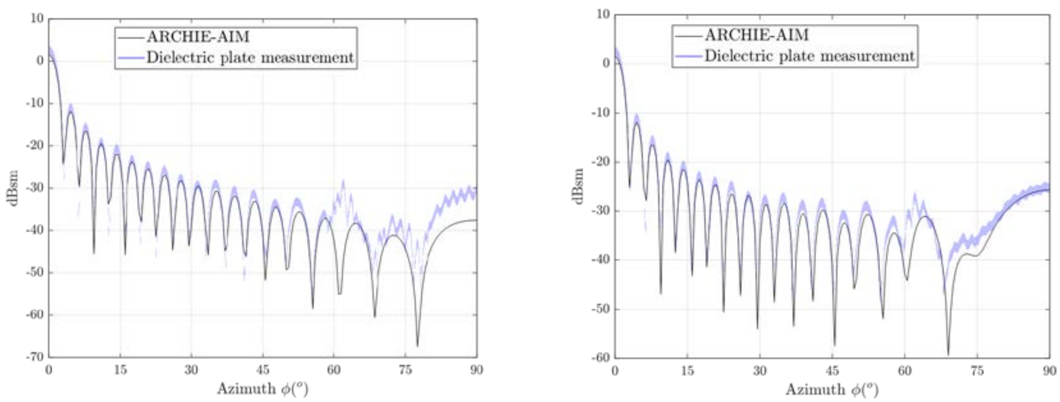

Figure 4: The HH ($\sigma_{\phi\phi,\mathrm{dB}}$, left) and VV ($\sigma_{\theta\theta,\mathrm{dB}}$, right) polarized RCS for the thin dielectric plate of width W = 6 in and frequency f = 10.24 GHz.

The above RCS results are that of the reference measurement and simulation data in the benchmark suite. The measurement data in the suite are the same as that shown in [1] and are plotted within a $\mp 1\ \mathrm{dB}$ window to represent the measurement uncertainties. The measured values differ significantly from simulated values near grazing incidence; as detailed in [1], this is because of a foam column maximum return occurring around $\phi = 60°$ and because of the low return of the dielectric plate, which render the coherent background subtraction technique used in the measurement insufficient to isolate the plate's RCS.

Notes

1. The measurement data are provided at every 0.25^{o} in the azimuthal range; the simulation data are at every 0.5^{o}.
2. The simulation data were calculated by using the ARCHIE-AIM code, a frequency-domain FFT-accelerated integral-equation solver developed at UT Austin [2]-[4], and are the same as the results in [1].

References

[1] J. T. Kelley, D. A. Chamulak, C. Courtney, and A. E. Yilmaz, "Increasing the material diversity in the Austin RCS Benchmark Suite using thin plates," in *Proc. Ant. Meas. Tech. Assoc. (AMTA) Symp.*, Nov. 2020.

[2] M. F. Wu, G. Kaur, and A. E. Yılmaz, "A multiple-grid adaptive integral method for multi-region problems," *IEEE Trans. Antennas Propag.*, vol. 58, no. 5, pp. 1601-1613, May 2010.

[3] F. Wei and A. E. Yılmaz, "A more scalable and efficient parallelization of the adaptive integral method part I: algorithm," *IEEE Trans. Antennas Propag.*, vol. 62, no.2, pp. 714-726, Feb. 2014.

[4] J. W. Massey, V. Subramanian, C. Liu, and A. E. Yılmaz, "Analyzing UHF band antennas near humans with a fast integral-equation method," in *Proc. EUCAP*, Apr. 2016.